ACCURACY OF IRIS RECOGNITION USING TRAPEZOIDAL TEMPLATES

A THESIS SUBMITTED TO

THE FACULTY OF ARCHITECTURE AND ENGINEERING

OF

EPOKA UNIVERSITY

BY

SARA KLLOGJRI

IN PARTIAL FULFILLMENT OF THE REQUIREMENTS

FOR

THE DEGREE OF MASTER OF SCIENCE

IN

COMPUTER ENGINEERING

JULY, 2022

Approval sheet of the Thesis

This is to certify that we have read this thesis entitled **"Accuracy Of Iris Recognition Using Trapezoidal Templates"** and that in our opinion it is fully adequate, in scope and quality, as a thesis for the degree of Master of Science.

_____

Dr. Arban Uka
Head of Department
Date: 04.07.2022

Examining Committee Members:

Dr. Igli Hakrama (Computer Engineering) _____

Dr. Shkelqim Hajrulla (Computer Engineering) _____

Dr. Arban Uka (Computer Engineering) _____

I hereby declare that all information in this document has been obtained and presented in accordance with academic rules and ethical conduct. I also declare that, as required by these rules and conduct, I have fully cited and referenced all material and results that are not original to this work.

Name Surname: Sara Kllogjri

Signature: _____

ABSTRACT

ACCURACY OF IRIS RECOGNITIONUSING TRAPEZOIDAL TEMPLATES

Sara Kllogjri

M.Sc., Department of Computer Engineering

Supervisor: Dr. Arban Uka

Authentication is the process of identifying someone or something and verifying its validity.There are a lot biometric technologies, which include finger scanning, finger vein ID, facial recognition, voice recognition, retina scanning, iris recognition etc. Being one of the most reliable methods, we have chosen to analyze iris recognition. Since it is unique, unchangeable and difficult to falsify, it is considered to be a great candidate for authentication. This process involves several steps – segmentation, normalization, encoding, matching. The quality of iris pictures noninheritable at-a-distance or below less strained imaging environments is understood to degrade the iris recognition accuracy. The periocular data is inherently embedded in such iris pictures and might be exploited to help within the iris recognition below such non-ideal situations. Our main aims in this thesis are new methods for the segmentation and encoding stages of the iris recognition using trapezoidal templates. Considering all the newly presented methods, we can say that they improve the performance of the algorithm for the CASIA database.

Keywords: Iris Recognition, Segmentation, Encoding, Accuracy, EER

ABSTRAKT

SAKTESIA E NJOHJES SE IRIS-IT DUKE PERDORUR MODELE TRAPEZOIDALE

Sara Kllogjri

Master Shkencor, Departamenti i Inxhinierisë Kompjuterike

Udhëheqësi: Dr. Arban Uka

Autentifikimi është procesi i identifikimit të dikujt ose diçkaje dhe verifikimi i vlefshmërisë së tij. Ka shumë teknologji biometrike të cilat përfshijnë skanimin e gishtit, ID-në e venave të gishtit, njohjen e fytyrës, njohjen e zërit, skanimin e retinës, njohjen e irisit etj. Duke qenë një nga metodat më të besueshme, ne kemi zgjedhur të analizojmë njohjen e irisit. Meqenëse është unike, e pandryshueshme dhe e vështirë për t'u falsifikuar, konsiderohet të jetë një kandidat i shkëlqyeshëm për identifikim. Ky proces përfshin disa hapa - segmentimin, normalizimin, kodimin, përputhjen. Cilësia e imazheve të irisit të marra në një distancë ose nën mjedise më pak të kufizuara të imazhit dihet që degradon saktësinë e njohjes së irisit. Informacioni periokular është ngulitur në mënyrë të natyrshme në imazhe të tilla të irisit dhe mund të shfrytëzohet për të ndihmuar në njohjen e irisit nën skenarë të tillë jo ideal. Qëllimet tona kryesore në këtë tezë janë metodat e reja për segmentimin dhe fazat e kodimit të njohjes së irisit duke përdorur modele trapezoidale. Duke marrë parasysh të gjitha metodat e paraqitura rishtas, mund të themi se ato përmirësojnë performancën e algoritmit për bazën e të dhënave CASIA.

Fjalëtkyçe: Njohja e iris-it, Faza e Segmentimi, Faza e Enkoding, Saktësia, EER

Dedicated to my family and friends!

ACKNOWLEDGEMENTS

I would like to express my special thanks to my supervisor Dr. Arban Uka for his continuous guidance, encouragement, motivation and support during all the stages of my thesis. I sincerely appreciate the time and effort he has spent to improve my experience during my graduate years.

TABLE OF CONTENTS

LIST OF TABLES

LIST OF FIGURES

CHAPTER 1

INTRODUCTION

1.1 Authentication

Security is an essential element in everyday life, including security in military units [Gold 2010], in banking system, in research centers etc. Face recognition, iris recognition, vein recognition, fingerprint recognition are all techniques that have been developed over the last decades.

Identification and validity verification are steps in the authentication process. When it comes to establishing a user's identification to the server in computer science, authentication is crucial. One of the most popular methods of authentication is the use of a password, which is done for security reasons. However, it has been demonstrated that some passwords are simple to forget, guess, or locate if you write them down anywhere, putting your sensitive data at risk.

Many studies have been conducted to develop a better authentication method in order to ensure the security of data, and biometric authentication is currently one of the top contenders. This includes ways to recognize a person's physiological characteristics, like finger prints and finger vascular

Biometric systems function in two distinct stages. A template is added to the database in the first stage. To do this, a sample of the feature, such as a sound signal for speech recognition or a digital image for face identification, is taken and mathematically turned into a biometric template. The database will store that template. The process of matching or identifying the person is the second stage. As mentioned above, a fresh template is produced for a particular feature. Up until a match is discovered, this template will be compared to every other template kept in the database.

Because these distinctive characteristics are very hard to forget, biometric verification has the advantage of preventing fraud and misuse. Additionally, it implies that you don't need to remember anything or write anything down because your biometric credentials are constantly with you.

1.2 Iris structure

For humans, the organ of sight is the eye. According to MedicineNet, Inc., it is made up of a variety of parts, including the cornea, iris, pupil, lens, retina, macula, optic nerve, choroid, and vitreous. The iris, however, plays the most significant role in our research.

The colorful portion of the eye known as the iris controls how much light enters the eye by separating the pupil, which is black in color, from the sclera, which is brilliant in color. The iris is a ring-shaped collection of elastic connective tissues that forms the eye's sumptuous pattern of intricate texture (N. Othman & B. Dorizzi 2013). While the barrier between the iris and sclera is known as the limbic boundary, the border between the iris and pupil is known as the pupillary.

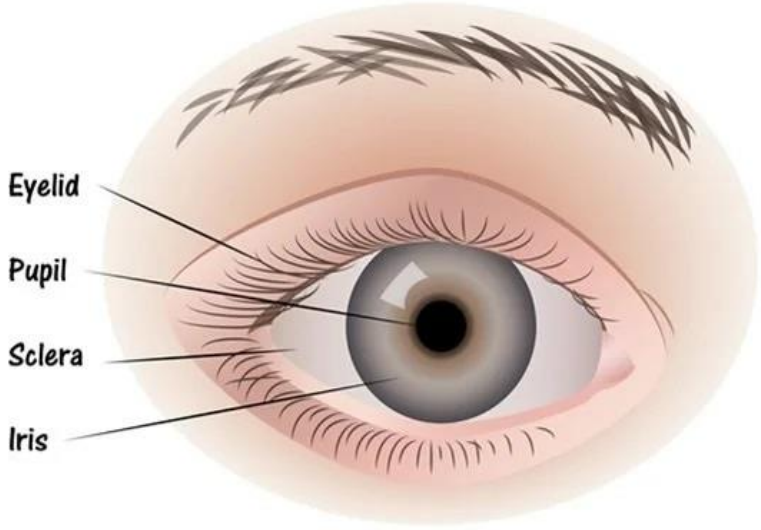

Figure 1 Human eye structure

https://www.news-medical.net/health/Anatomy-of-the-Human-Eye.aspx

1.3 Iris recognition

One of a person's physical traits that is distinctive, simple to spot, well-protected (an internal organ), and constant over the course of a lifetime is their iris. Additionally, it cannot be surgically changed without endangering vision (G, Thapliyal, &Sethi, 2012). Its epigenetic pattern is completely random and complex, according to studies. The texture of the iris in the left eye is different from the texture in the right eye not only in monozygotic twins but also in the same individual.

Identifying the iris is the initial step in the iris recognition procedure. We are able to retrieve the digitalized image of the eye using image processing methods. Then, using the circular Hough transform method and the parabolic Hough transform technique, we can pinpoint the pupil, iris, and eyelids, respectively (Efford, 2000). Once this region has been localized, a biometric template must be made that includes a mathematical representation of the distinctive data kept in an iris.

When someone wants to be recognized by an iris recognition system, his eye will first be photographed and the template will be saved in a database. Once a template has been produced as previously explained, it will be compared to every other template that is kept in the database. If the similarity between the present template and one of the templates in the database is extremely near to 100 percent, these templates are taken to be belonging to the same person because the system has the ability to reject or approve the individual (Bowyer &Kuehlkamp 2016). If a lower level of resemblance is discovered, it indicates that the person is not present in the database.

1.4 Thesis purpose

The purpose of this thesis is to examine a system that uses tapezodial templates to assess iris patterns to identify persons. A brief review of the theoretical ideas and steps involved in iris identification, such as segmentation, normalization, encoding, matching, etc., may be found here.

The goal is to run several experimental tests using a trapezoidal iris template to determine the relationship between accuracy and EER with the number of people

and the number of photos taken for each person using the trapezoidal template for iris recognition, using prior research that has been done in this field using the traditional rectangular template as well as previously written codes.

CHAPTER 2

LITERATURE REVIEW

2.1 CASIA database

The most popular database for iris recognition is the CASIA database (Chinese Academy of Sciences - Institute of Automation), which is the database we used for our studies. There are seven iris photos for each of the 108 people. The pictures are taken under infrared light, which doesn't reflect anything (Chinese Academy of Sciences, 2003). Each eye image has a resolution of 320 x 280 pixels and is recorded in bitmap format.Other iris databases are the other versions of CASIA databases with at least 3more versions. The more recent versions (of CASIA) include iris image fromdifferent eyes, where one can also test the similarity between two eyes of the sameindividual. IIT (Indian Institute of Technology) is also another database used in theliterature. UBIRIS [Proenca& Alexandre, 2005].

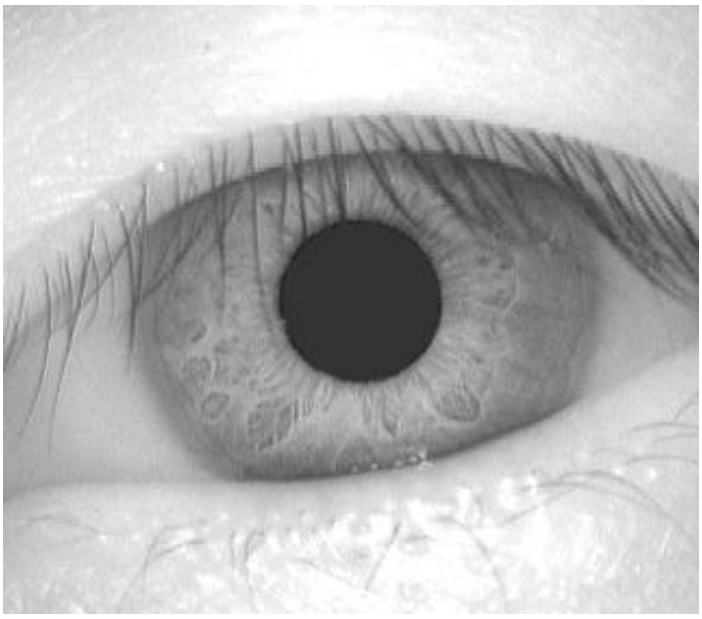

Figure 2.*Example of iris image from CASIA database (person 7, pic no.2*

2.2 Segmentation

The initial phase in the iris identification process is segmentation. Its goal is to identify the iris region in the provided eye photos. The area between the pupil and sclera is known as the iris, as we already stated. Two concentric circles can be used to depict it (respectively pupillary and limbic boundaries). The Hough Transform method allows us to find the iris. However, a given image might occasionally include noises like light reflections or even eyelids and eyelashes (Efford, 2000).

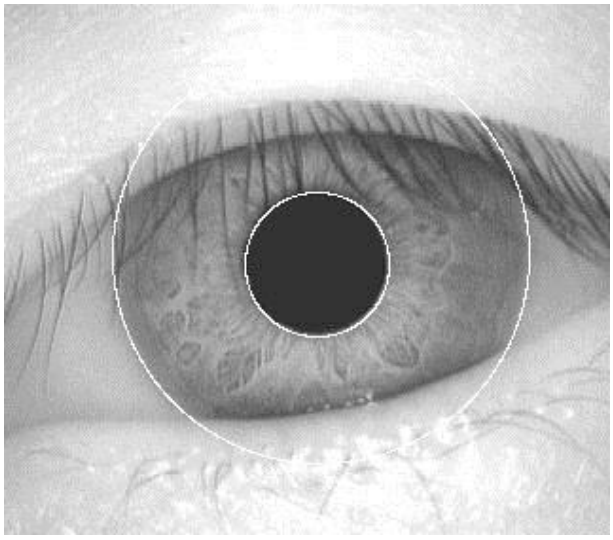

Figure 3.Example of iris image segmented (person 7, pic no.2)

2.2.1 Hough transform

We may calculate the parameters of basic geometric objects like lines and circles that may be present in a picture using the Hough transform algorithm. While the parabolic Hough transform technique can be used to identify eyelids, the circular Hough transform algorithm can be used to determine the center coordinates and radius of the pupil and iris. The process begins by creating an edge map using the first derivatives of the pixel values, and the output is then thresholded. In this manner, it locates the two circles that the iris is situated between. The eyelids are detected by the derivatives in the horizontal direction, and the iris is detected by the derivatives in the vertical direction (Efford, 2000) Pan and Xie (2005).

2.2.2 Detection of Noise in Iris Images

For the detection of eyelashes, Kong and Zhang have presented their own method. They have divided eyelashes in two groups, separable eyelashes and multiple eyelashes. To detect the ones that fall in the first group, 1D Gabor filters are used, since the convolution of a separable eyelash with the Gaussian smoothing function results in a low output value. To detect the ones that fall in the second groups, the variance of intensity is used. If the variance of intensity values in a small window if lower than a threshold, the center of the window is considered as a point in an eyelash.

2.2.3 Classical & improved segmentation (S1& S3)

The iris and pupil radius ranges in the Casia Database are, respectively, 80 to 150 pixels and 26 to 75 pixels (Masek, 2003). According to Masek's algorithm, the circle separating the iris from the sclera is discovered first, followed by the circle separating the iris from the pupil. The radius of the pupil and iris as well as the (x,y) coordinates of their centers are two of the six parameters produced by this technique. (Masek 2003).

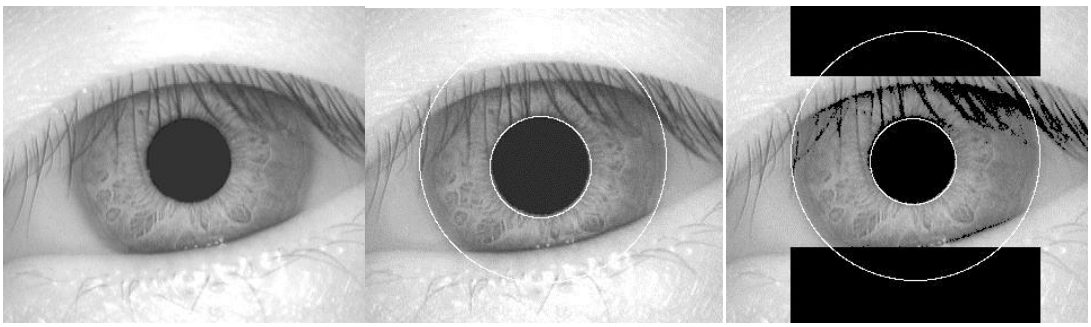

a) (b) (c)

Figure 4a) normal eye; (b) localization of pupillary and limbic boundaries; (c) noise detection (person 7, pic no. 2)

Due to the tiny variation in intensity values between the sclera and the iris in some of the photos, S1 produces some incorrect findings; as a result, changes were made to the segmentation method. Since the difference in intensity values is bigger than in Masek's method, the boundary between the pupil and the iris will be allocated first in S3. The limbic boundary will then be located using that circle as a guide. That collection of circles is still obtained using Hough's transform.If there is a significant pixel variation from concentricity, those circles are not taken into account. The circles in the remaining set will then be arranged according to how many edge points there are in the Canny edge map. A parameter (d3) will be applied to each circle in order to remove any unreliable circles. A circle will not be included if its parameter (d3) is greater than 25 pixels. (Uka*et al.*, 2017).

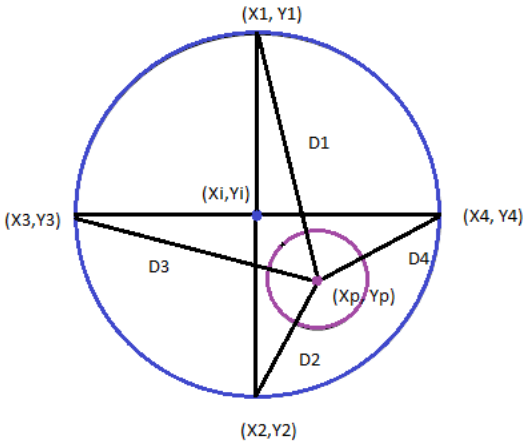

Figure 5. *Ilustration of d3 distance. The deviation of the iris center with respect tothe pupil center (Uka, 2017)*

The new method firstly finds boundary of the pupil instead of boundary of iris, and then finds the outer iris boundary of the iris.[Liu et al.] in their work, used this new optimization technique and reported that it improved the accuracy of the iris recognition system. Recently, Uka et al.used state-of-art segmentation technique which is called segmentation technique S3 and denoted as EPK_IRIS.

2.2.4Adding Noises

The variety of individuals, the sort of camera and wavelength accustomed to capture the image, the relative strength within the background, the interference with the eyelids and eyelashes square measure all factors which will have an effect on negatively one or a lot of of the procedures that square measure performed in iris recognition. underneath the mentioned truth, we tend to degrade image qualities by adding artificial noises to the CASIA dataset. Two sorts of noises we have a tendency to use two sorts of noises such as Gaussian noise and Salt-and-pepper noise.When we add artificial Gaussian noise, and Salt-andpepper noise to the CASIA iris dataset, we reported that S3 segmentation (EPK_IRIS) always gives better segmentation results than S1(Masek) segmentation where could be seen in Figure 6 and Figure 7.

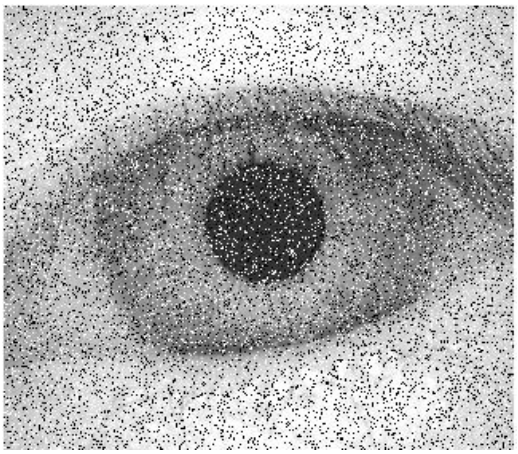

Figure 6, Person 7, Image 2, Salt-and-Pepper Noise

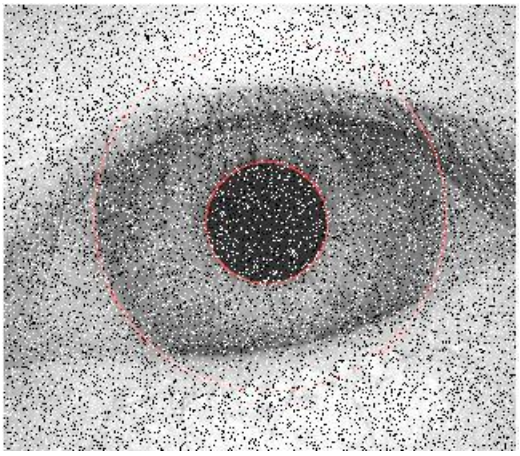

Figure 7, Person 7, Image 2, Salt-and-Pepper Noise Segmentation

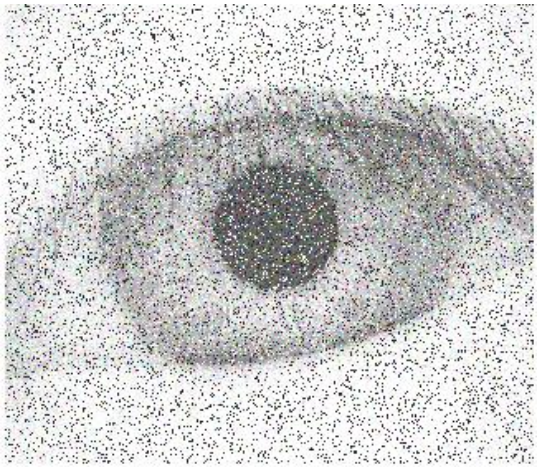

Figure 8, Person 7, Image 2, Gaussian Noise

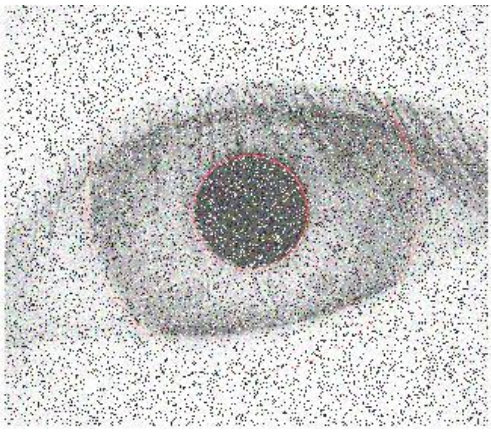

Figure 9, Person 7, Image 2 Gaussian Noise Segmentation

2.3 Normalization

The second phase in the iris recognition process is normalization. We want to have an extracted iris template after localizing the iris that can be compared to other irises (Daugman J., 1994). We try to correct these inconsistencies with normalization. Different head postures, imaging distance, iris stretching induced by pupil dilation during light intensity change, or rotation of the eye within the eye socket may lead to dimensional inconsistencies. This will produce iris regions with the same constant dimensions so that similar details in two images of the same iris taken under different lighting circumstances will appear at the same spatial location (Masek 2003).

(a) (b)

Figure 10. *(a) iris region; (b) iris region mask after normalization process*

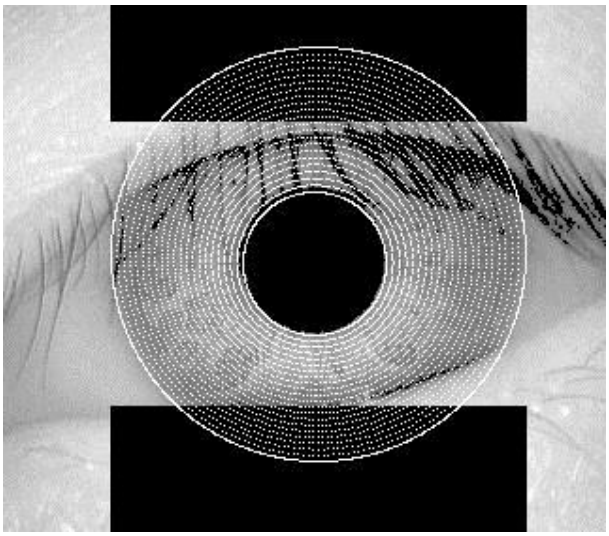

Figure 11Person 7, Image 2 after Normalization process

2.3.1 Daugman’s rubber sheet model

We utilize Daugman's rubber sheet model to achieve a successful normalization procedure. Polar coordinates of the type (r,), where r belongs to [0,1] and belongs to [0,2], are used to represent each point on the iris. This approach takes into account the irregularities brought on by dilated pupils, various imaging distances, or non-concentric pupil and iris. The iris template is moved in one direction at a time until it is composed to be compared to control iris rotation (Daugman J., 1994). (Johar& Kaushik, 2015).

2.4 Encoding

The third phase in the iris recognition process is encoding. It is used to produce biometric templates that contain an iris' distinctive characteristics. To provide the most reliable identification of the person, just the most crucial information from the iris is encoded. Then, this developed biometric template is applied to template comparisons (Masek 2003).

2.4.1 1D Gabor filter

We use 1D Gabor filters to extract the most significant distinctive elements from an iris pattern. They provide the best simultaneous spatial and frequency representation of a signal. A sine function may be localized perfectly in frequency but not in space, hence the Gaussian modulation is employed to localize the sine function in both space and frequency. A signal can be divided into its symmetric component a quadrature pair of Gabor filters described by a cosine using Gaussian modulationand its odd component, which is, in this example, an imaginary part specified by a sine using the same modulator.The filter's center frequency is determined by the sine/cosine function's frequency, and its bandwidth is determined by the Gaussian's breadth (Masek, 2003).

2.4.2 Classical (E1) & Improved (E3) method for encoding

Each phaser will be given two bits and will be quantized into one of the complex plane's four quadrants. Two adjacent regions' bit patterns are 50% different

from one another. The encoded template that is created will be 20x480 in size. If there are any iris regions where the phase information's amplitude is zero, those regions are regarded as belonging to the noise mask. The noise bits in this template will be assigned to bit 1 in the same manner as previously described dimenions.

With this change, the complex plane will now be split into 8 areas, each of which will be represented by 4 bits of information. Pair regions' bit patterns differ by 25%, and the opposite regions' bit patterns differ by 100%. The encoded template will be 20x720 in size.

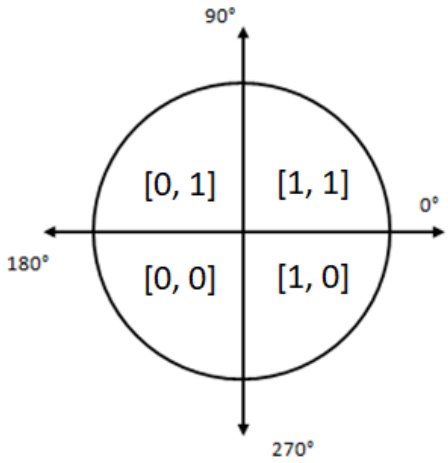

Figure 12. *Different Four quantization levels of phase space*

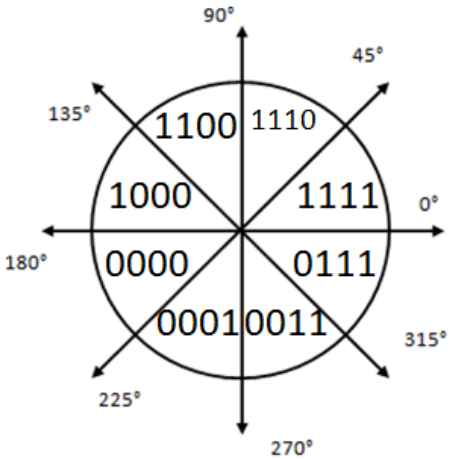

Figure 13. *Different Eight quantization levels phase space*

2.5 Matching

The process of iris recognition ends with matching. A matching metric that measures how similar two iris templates are must be generated after the encoding stage to complete the template generation process. Comparing templates from the same iris is known as intra-class comparison, whereas doing so with different irises is known as inter-class comparison. For the comparison to be confident and provide an accurate result, the metric range of values for these two classes must be distinct and not overlap (Rathgeb, Uhl, & Wild, 2013).

The following formulas are used to calculate the number of intraclass and interclass comparisons:

$$N_{intra} = N \cdot \frac{n!}{(n-2)! \cdot 2!}$$ ***Equation 1.***

$$N_{inter} = n^2 \cdot \frac{(N-1) \cdot N}{2}$$ ***Equation 2.***

where N is the number is the number of people in database and n is the number of iris images for each person.

2.5.1 Hamming distance

Hamming distance is employed as the matching metric in the matching phase (Daugman J., 1994). This method counts the same bits between two bit patterns in order to determine whether or not they are from the same iris.

Hamming distance is calculated as below:

$$HD = \frac{1}{N - \sum_{k=1}^{N} Xn_k (OR) Yn_k} \sum_{j=1}^{N} X_j (XOR) Y_j (AND) Xn'_j (AND) Yn'_j$$

Equation 3. *Hamming distance calculation*

where Xj and Yj are the two bit-wise templates to compare, Xnj and Ynj are the corresponding noise masks for Xj and Yj, and N is the number of bits represented by each template (Masek 2003).

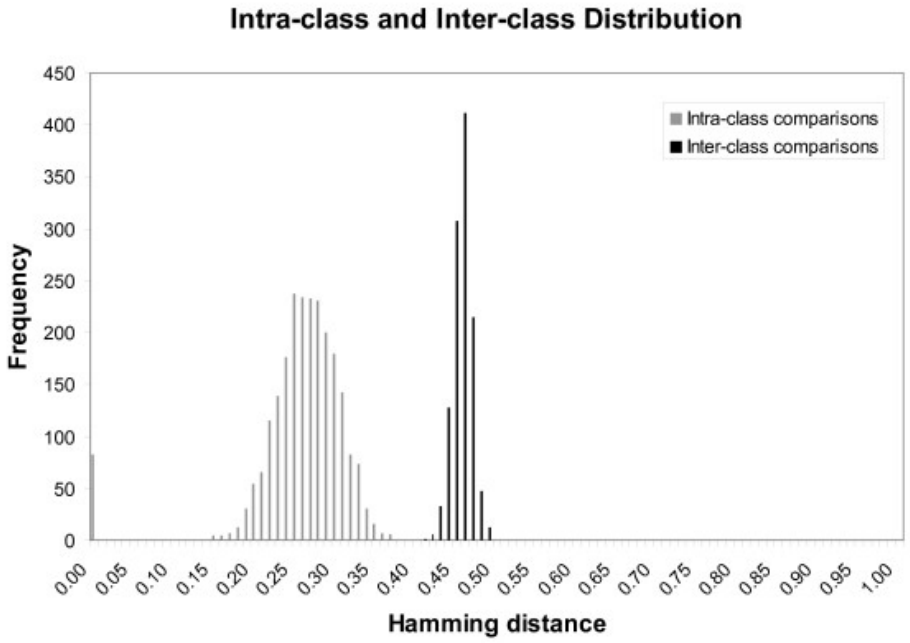

Figure 14. *Inter-class and Intra-class distribution*

https://www.researchgate.net/figure/Hamming-distance-distributions-Intra-class-same-subjects-and-inter-class-different_fig5_44901004

2.5.2 DOF (Degrees of freedom)

The degrees of freedom, DOF is conducted to determine theuniqueness of the iris templates. We can calculate it by using the mean and standarddeviation of the inter class value distributions. The degrees of freedom is calculatedwith no shifting process while finding the Hamming Distance.

$$DOF = \frac{\mu_{inter}(1-\mu_{inter})}{\sigma_{inter}^2}$$

Equation 4. *Degrees of Freedom*

The theoretical value of DOF concludesthat the iris image pixel intensity values to be compleately random and equal to the number of pixels that are gathered in the normalization step times the number of bits per pixel. The number of pixels is equal to the radial resolution times the angular resolution. The encoding methodwhich is used the most is the one that was used originally by Daugman, which assigns two bits per pixel. In this work, the phase space is separated into more than four quadrants so more pixels are selected. The speculation proposed here is that by decreasing the FAR, a higher DOF would produce two different templates with a higher accuracy. From the interclass histogram can be calculated the experimental DOF (DOF^{exp}) of the dataset. DOF^{exp} is smaller than DOF^{th} since the pixel values have some inherent correlation. (Koç *et al.*, Uka 2019)

Decidability, d - prime is another metric to measure the separation of inter and intra class distribution which depends on the mean and standard deviation of these values. The greater the decidability, the greater the separation of inter and intra class distribution, the more accurate the recognition.

$$d\ prime = \frac{|\mu_{intra} - \mu_{inter}|}{\sqrt{\frac{\sigma_{intra}^2 + \sigma_{inter}^2}{2}}}$$

Equation 5. Decidability, D Prime

2.6 Performance of biometric systems

In the identification scenario, an individual claims to have a particular identity and the biometric system verifies this identity. If the the match of the two samples isgood enough, the claim is accepted, otherwise it is rejected. The possible outcomesof the identification scenario are: i)true positive (TP) – when there is a correct match between anunknown sample and a sample stored in the database, ii) true negative (TN) – when there is a correct mismatch between anunknown sample and a sample stored in the database, iii) false positive (FP) – when there is an incorrect match between anunknown sample and a sample stored in a database,

iv)false negative (FN) – when there is an incorrect mismatch between an unknown sample and sample stored in a database.

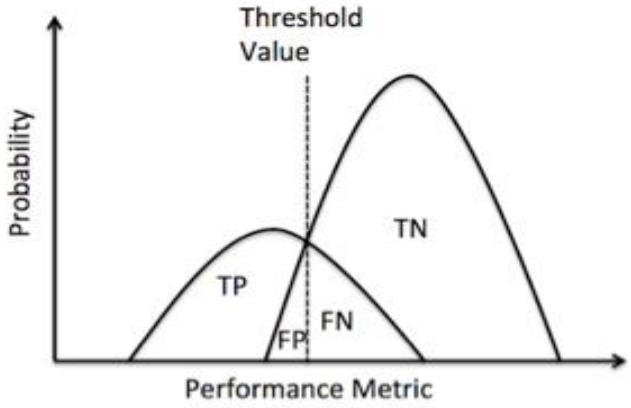

Figure 15. *Performance metric parameter*

In order to determine whether an image is already stored in database FRR and FAR are used.

- False Accept Rate (FAR) – measures the percentage of invalid inputs being accepted.
- False Reject Rate (FRR) – measures the percentage of valid inputs being rejected.
- Equal Error Rate (ERR) – the rate at which both FAR and FRR are equal. It is obtained from ROC (Relative Operating Curve) plot by taking the point where FAR and FRR meet (Figure 16. EER, FAR and FRR intersection point). The lower the EER, the more accurate the system is considered to be. (Ranjan, et al. 2009)

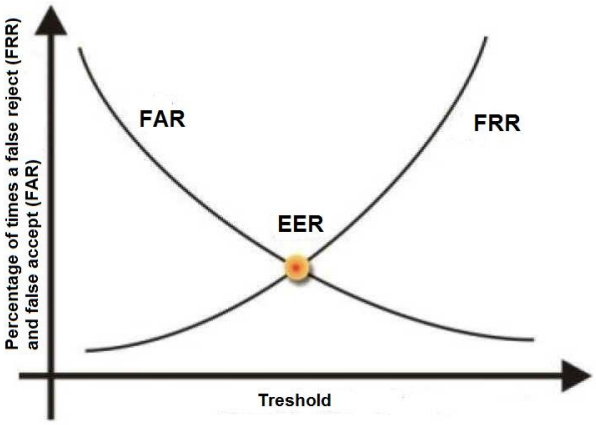

Figure 16. *EER, FAR and FRR intersection point*

For iris recognition systems, main goal is achieving always more accurate results. Maximum accuracy could be done by maximizing sum of true positive (TP) and true negative (TN) values. This yields thatthe accuracy and the EER are never instantaneously at their optimal value for the same threshold value [13], therefore in different research papers, we see confusing results that are reported. In general, the FAR and the FRR results are always inversely proportional. If False Accept Rate and False Reject Rate results are equal to zero, then we have a absolutely perfect biometric system since the results yields also equal error rate is also zero.

CHAPTER 3

METHODOLOGY

As we mentioned earlier, the aim in our study was to find the relation of the accuracy and EER with the number or people and the number of photos taken for each person. To find this relation, we had to run the code several times, while changing the n and N using rectangular and trapezoidal template. We made the same experimental tests for S1_E1, S3_E1 and S3_E3 and we recorded the results, so we could analyze them later. We do the same thing after implementing Gaussian Noise & Salt-and-Pepper Noise to compare them and see which one has better results.

The most important calculations that we had to make during this process were: inter-class comparisons, intra-class comparisons, FAR, FRR, EER and accuracy.

To calculate the number of intra-class comparisons we used the equation shown inEquation 1. On the other hand, to calculate the number of inter-class comparisons we used the equation shown in Equation 2. These two calculations are really important, and they are used later to calculate the accuracy.

The next calculations that we needed to do were FAR and FRR.

FAR can be calculated as:

$$FAR(n) = \frac{Number\ of\ successful\ imposter\ attempts\ for\ a\ qualified\ individual\ n}{Total\ number\ of\ imposter\ attempts\ for\ that\ qualified\ individual\ n}$$

and

$$\boldsymbol{FAR = \frac{1}{N}\sum_{n=1}^{N} FAR(n)}$$

Equation 7. *FAR*

FRR can be calculated as:

$$FRR(n) = \frac{Number\ of\ rejected\ verification\ attempts\ for\ a\ qualified\ individual\ n}{Total\ number\ of\ verification\ attempts\ for\ that\ qualified\ individual\ n}$$

and:

$$\boldsymbol{FRR = \frac{1}{N}\sum_{n=1}^{N} FRR(n)}$$

Equation 8. *FRR*

To find the EER, we had to plot the values (in percentage) of FAR and FRR and the intersection of those two lines gave us the value of the EER, as shown in *Figure 16.* EER, FAR and FRR intersection point

The last calculation that we had to make was the accuracy. Accuracy can be calculated as:

$$\boldsymbol{Accuracy = \frac{TP \cdot intra + TN \cdot inter}{inter + intra} \cdot 100\%}$$

Equation 9. *Accuracy*

Another extra calculation that we can make is the ratio between the inter and intra class comparisons.

$$\boldsymbol{\frac{N_{inter}}{N_{intra}} = \frac{n^2 \cdot \frac{(N-1)\cdot N}{2}}{N \cdot \frac{n!}{(n-2)!\cdot 2!}} = \frac{n \cdot (N-1)}{(n-1)}}$$

Equation 10. *Ratio between inter and intra*

We used this formula to plot the graphs showing how the ratio between inter and intra class comparisons changes for different number of people while using the same number of images per person.

Trapezoidal Template Creation

In the stage of encoding we create an iris template by using different quantization techniques based on intensity values or phase information. In the rectangular template, which is widely used for iris recognition process, the ‘pixel intensity template’ has a size of 20x240. Meanwhile, in our work we modified it by redesigning the iris template as a trapezoidal-shaped template. Here, the upper and the shortest base of the trapezoid correspond to the smallest circle that is closest to the pupil and the lower base of the trapezoid corresponds to the largest circle that is at the boundary between the iris and the sclera. With this technique, a 20x468 "pixel intensity template" is produced. The size of the "phase information template" doubles in length to become 20x936 when we calculate phase information using two bits of data in the form of 11, 01, 00, and 10 for each phasor. Since we have a larger template with more pixel values to be evaluated, a larger number of degrees of freedom can be generated, and this is expected to produce a higher accuracy and a lower equal error rate. [Koc et al., 2018]

CHAPTER 4

RESULTS AND DISCUSSIONS

We examined the S1 and S3 methods of segmentation as well as the E1 and E3 methods of encoding using random datasets from the CASIA database in order to compare the accuracy and EER for each of them. S1 and S3 were compared first using the E1 method of encoding, and E1 and E3 were compared second using the S3 method of segmentation. The tests were conducted in the manner that is detailed below.

First, we took three iris photos for 25 randomly selected individuals for each combination of segmentation and encoding methods (S1 E1, S3 E1, S3 E3) that we have taken into consideration. Then, we increased the number of photos per individual to 5 and 7, while maintaining the same number of participants. The same exams were administered to 50, 75, and 100 individuals. We determined the accuracy and EER for each test. The iris photos that we used for these tests were chosen at random, without any consideration of whether they were good or awful.

To graphically illustrate the relationship between the N and n for the EER values in S1 E1, S3 E1, and S3 E3, the findings for the aforementioned tables can also be shown as graphs. The horizontal axis in the following graphs reflects the average number of photos per individual (n), and the vertical axis the ratio of intra class comparisons to inter class comparisons. We've utilized bubbles to represent EER, with a bubble's radius representing the EER percentage.

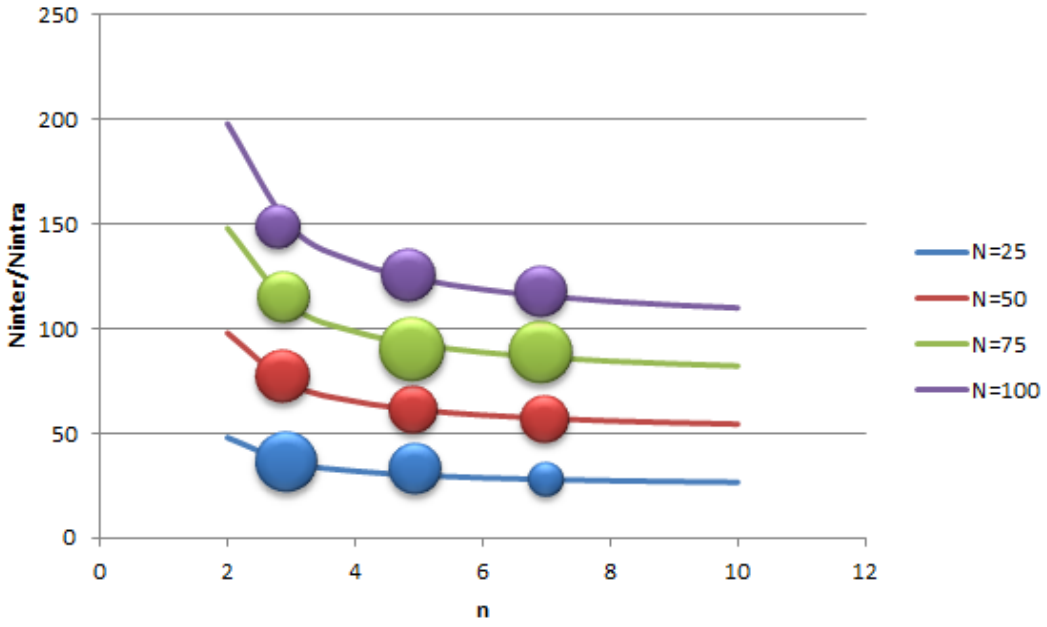

Figure 17. *EER as a function of size of dataset using S1_E1 (Qirko , 2018)*

A scale factor of 10 is employed in the following graph since the EER ranges from 1.91 percent to 3.468 percent (very significant compared to S3). The radius of thebubble, for instance, is 0.29 if the value of EER is 2.937 percent.

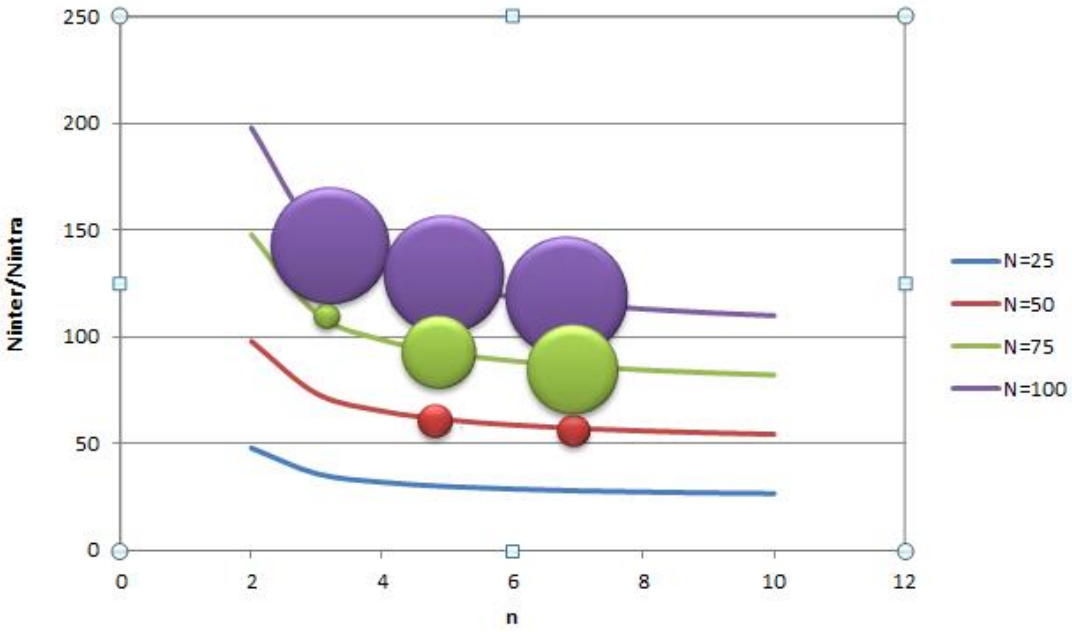

Figure 18. *EER as a function of size of dataset using S3_E1 (Qirko, 2018)*

Since the EER ranges from 0% to 0.717% in the graph above, a scale factor of 1 is applied. The radius of the bubble, for instance, would be 0.15 inches if the EER value were 0.1502 percent.

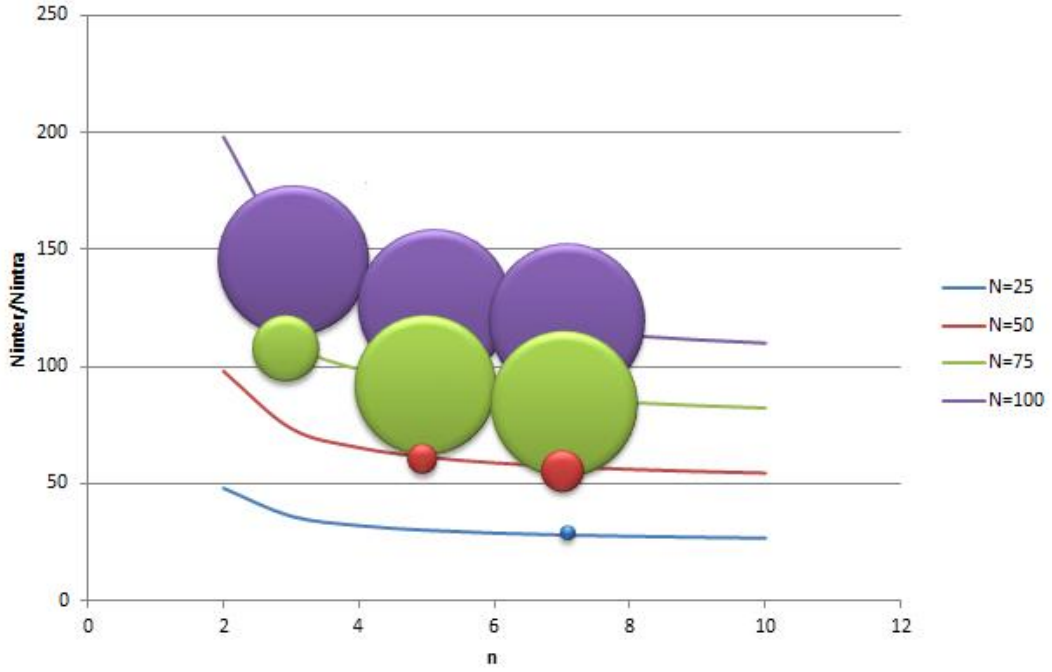

Figure 19. *EER as a function of size of dataset using S3_E3 (Qirko, 2018)*

A scale factor of 1 is used in the above graph because the EER ranges from 0% to 1.033%. The radius of the bubble, for instance, is 1.001% if EER is 1.001%.

The results shown above were obtained using the same random group of individuals who each had a different number of iris photographs taken. In addition to these experimental tests, we also conducted several additional using a random sample of individuals while maintaining the same number of participants and the number of photos per participant. The mean and standard deviation of EER were computed based on the findings.

Table 1. Accuracy and EER for N=25 and n=3

N=25	Sets	Accuracy	EER
n=3	1	100%	0%
	2	100%	0%
	3	99.9001%	1.281%
	4	99.9001%	2.53%
	5	99.9332%	0.3534%
	Mean	99.9467	0.8329
	Stdev	0.0505	1.0838

Table 2. Accuracy and EER for N=25 and n=5

N=25	Sets	Accuracy	EER
n=5	1	100%	0%
	2	99.9881%	0.3804%
	3	99.8807%	1.592%
	4	99.9046%	1.922%
	5	99.9803%	0.381%
	Mean	99.9507	0.8551
	Stdev	0.0542	0.8460

Table 3. Accuracy and EER for N=25 and n=7

N=25	Sets	Accuracy	EER
n=7	1	99.9934%	0.1001%
	2	99.9818%	0.5506%
	3	99.8604%	1.602%
	4	99.9211%	1.281%
	5	99.9803%	0.381%
	Mean	99.9474	0.7829
	Stdev	0.0562	0.6326

For the tables above, we have created graphs for mean and standard deviation.

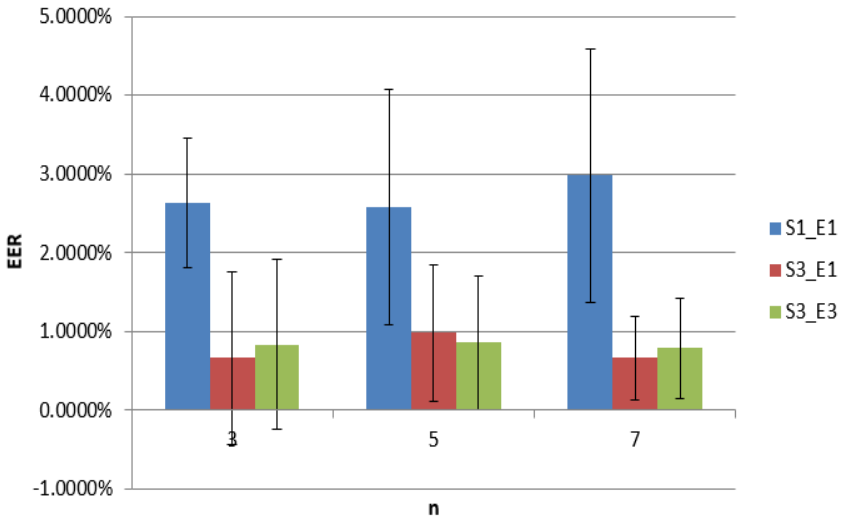

Figure 20.*Mean and standard deviation for N=25 (Qirko, 2018)*

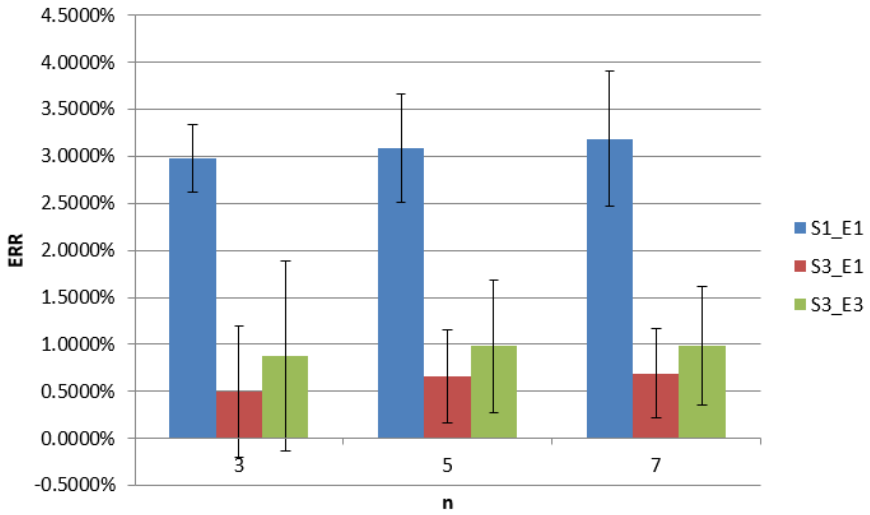

Figure 21. *Mean and standard deviation for N=50 (Qirko, 2018)*

After that we do the same experiments using trapezoidal template, this time we use only the segmentation S3 which is the one that has given better results in rectangular type template. We do the experiments by selecting different people images grouping them by 25, 50 & 75 and repeating the experiment 5 times per each taking random pictures from dataset.

In the tables below I have presented the results of the experiment showing n (number of pictures per person), N (number of people selected and which of the pictures are considered from 108 people that we have in CASIA database), accuracy,EER(Equal error rate) and DOF (Degrees of Freedom).

Table 4. Accuracy, EER and DOF for N=25 and n=7

N=25	Sets	Accuracy	EER	DOF
n=7	1	99.871%	3.6000%	3.54E+03
	2	99.7236%	3.3333%	3.51E+03
	3	99.6541%	3.8135%	3.56E+03
	4	99.7615%	1.3120%	3.21E+03
	5	99.6661%	3.0770%	3.31E+03
	Mean	99.73526%	3.0272%	3.42E+3
	Stdev	0.0875%	0.9981%	0,15E+3

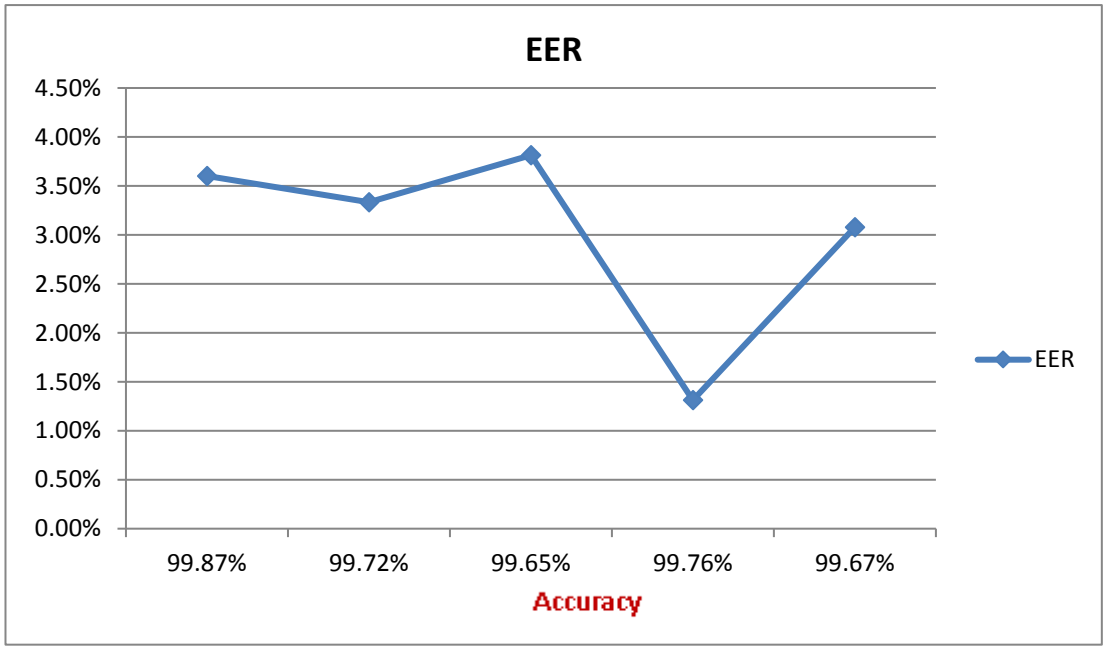

Figure 22. Accuracy and EER for N=25 and n=7

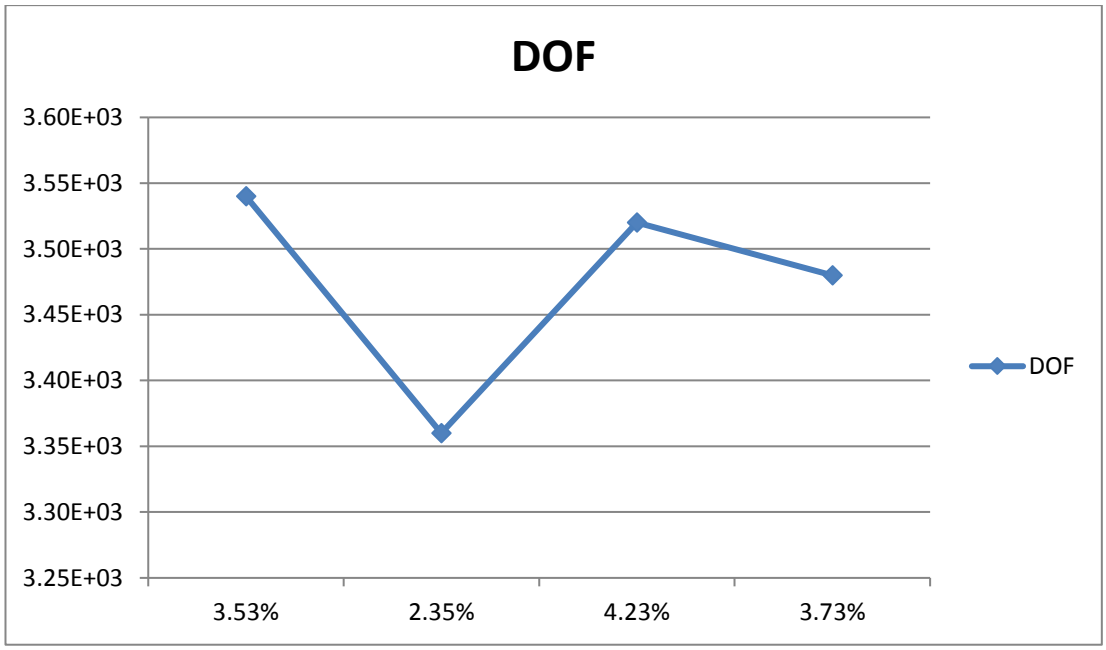

Figure 23, EER and DOF for N=25 and n=7

Table 5. Accuracy, EER and DOF for N=50 and n=7

N=50	Sets	Accuracy	EER	DOF
n=7	1	99.8796%	3.5294%	3.54E+03
	2	99.8394%	2.3530%	3.36E+03
	3	99.8485%	4.2310%	3.52E+03
	4	99.8240%	3.7255%	3.48E+03
	5	99.8307%	2.8850%	3.52E+03
	Mean	99.8444%	3.3448%	3.48E+3
	Stdev	0.0217%	0.7348%	0,07E+3

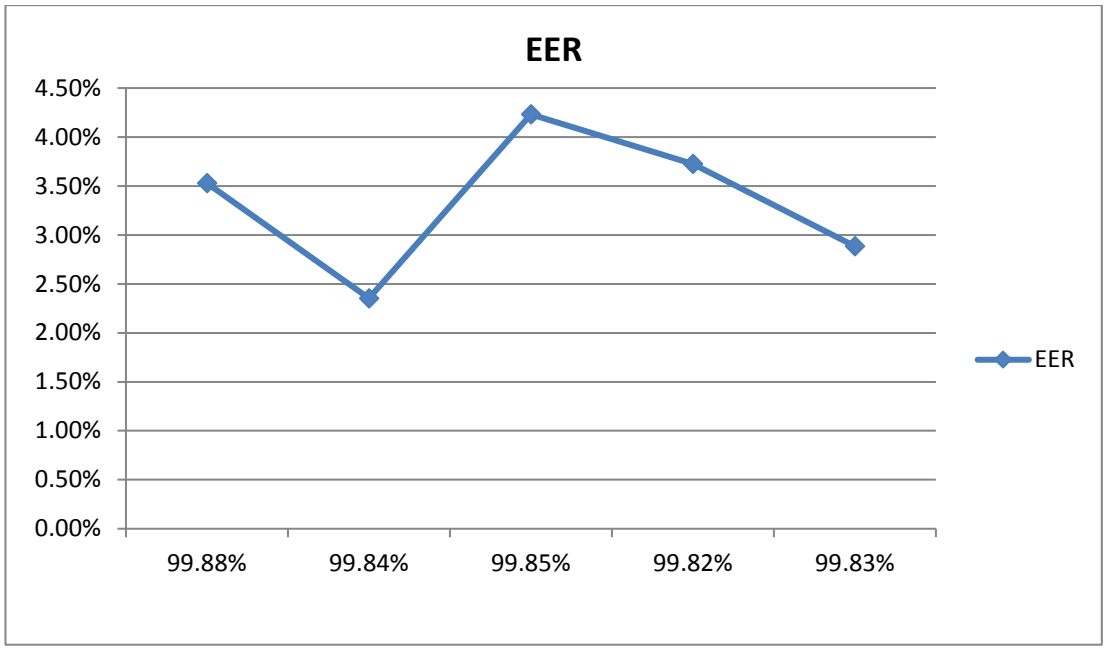

Accuracy

Figure 24. Accuracy and EER for N=50 and n=7

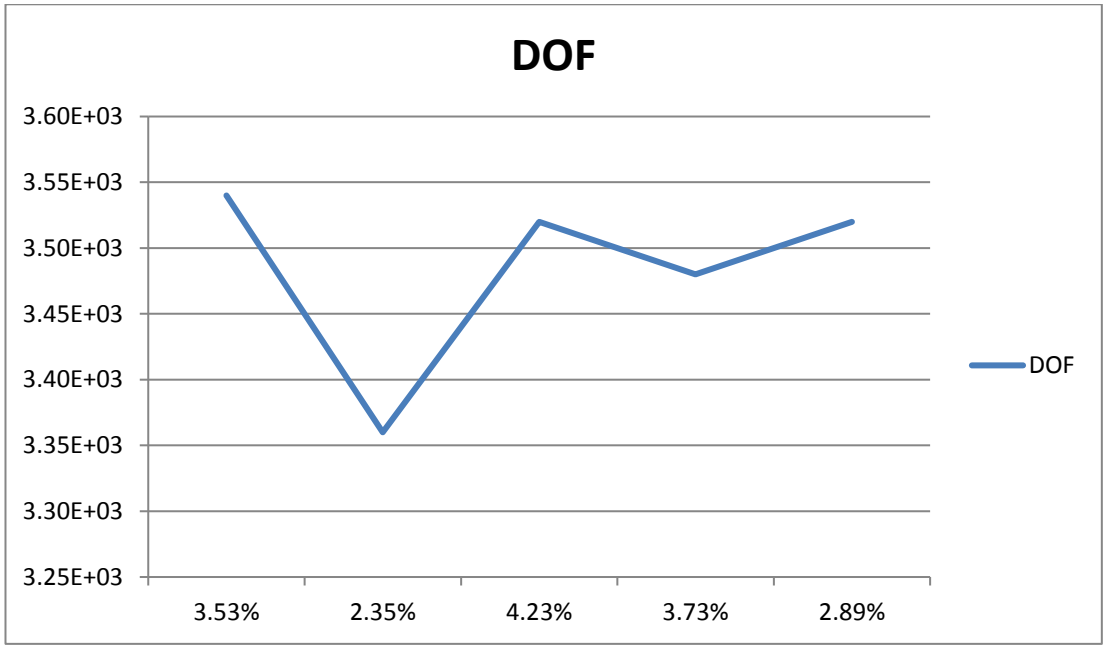

Figure 25. EER and DOF for N=50 and n=7

Table 6.Accuracy, EER and DOF for N=75 and n=7

N=75	Sets	Accuracy	EER	DOF
n=7	1	99.8988%	3.7335%	3.48E+03
	2	99.9000%	3.5525%	3.54E+03
	3	99.8999%	3.1169%	3.55E+03
	4	99.8999%	2.7272%	3.53E+03
	5	99.8667%	2.7272%	3.53E+03
	Mean	99.8931%	3.1715%	3.52E+3
	Stdev	0.0147%	0.4634%	0.02E+3

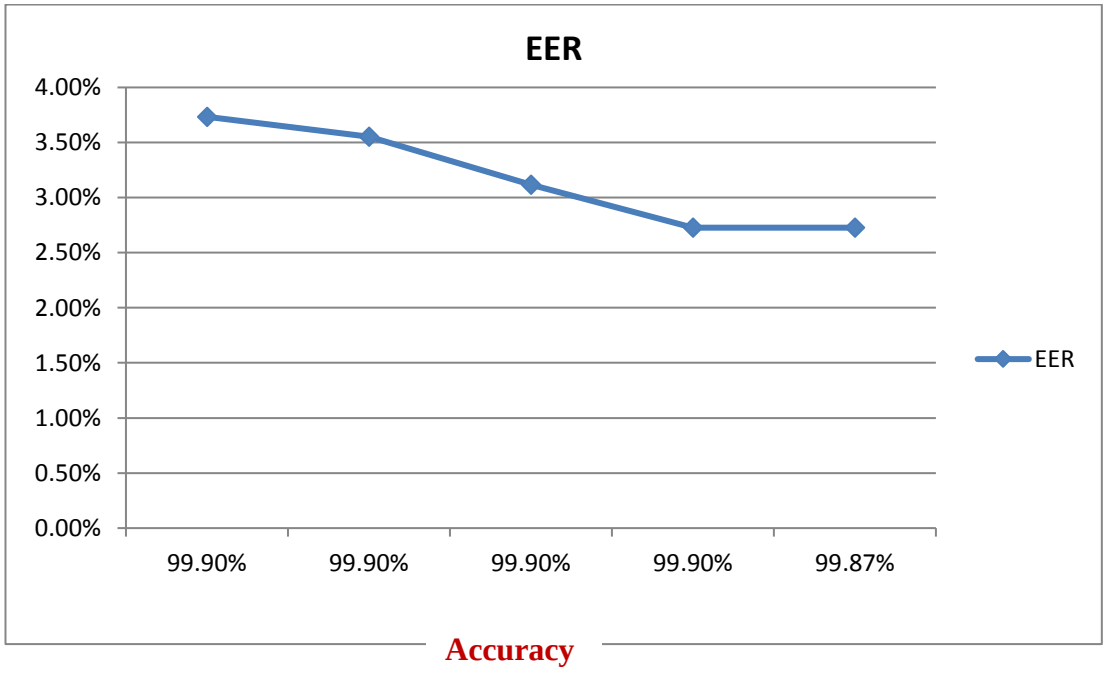

Figure 26. Accuracy and EER for N=75 and n=7

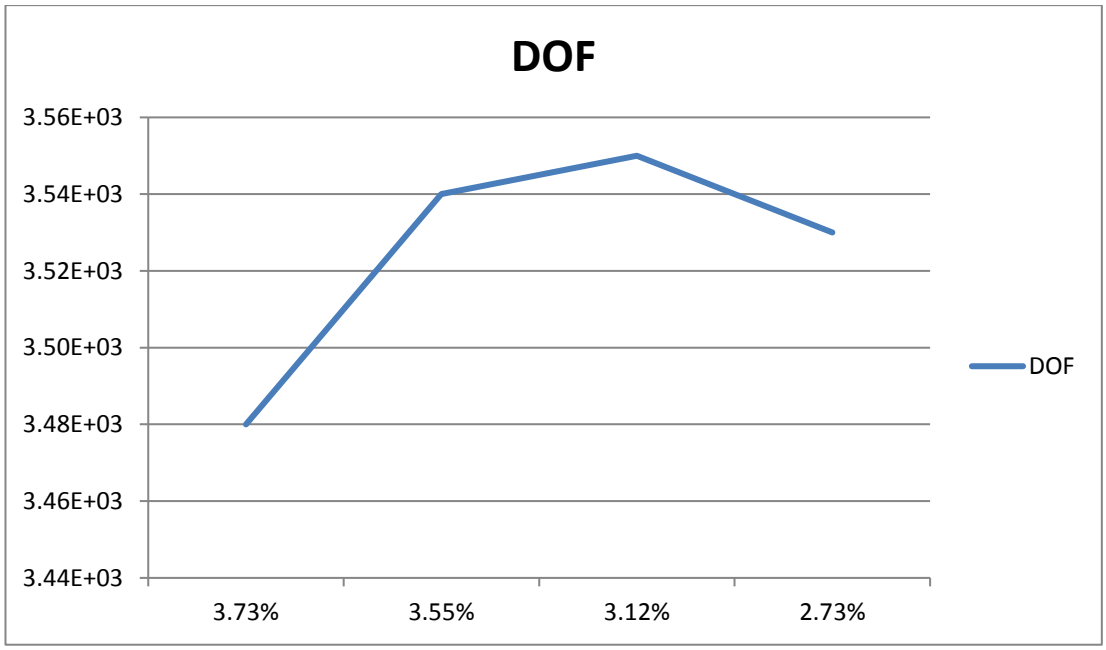

Figure 27. EER and DOF for N=25 and n=7

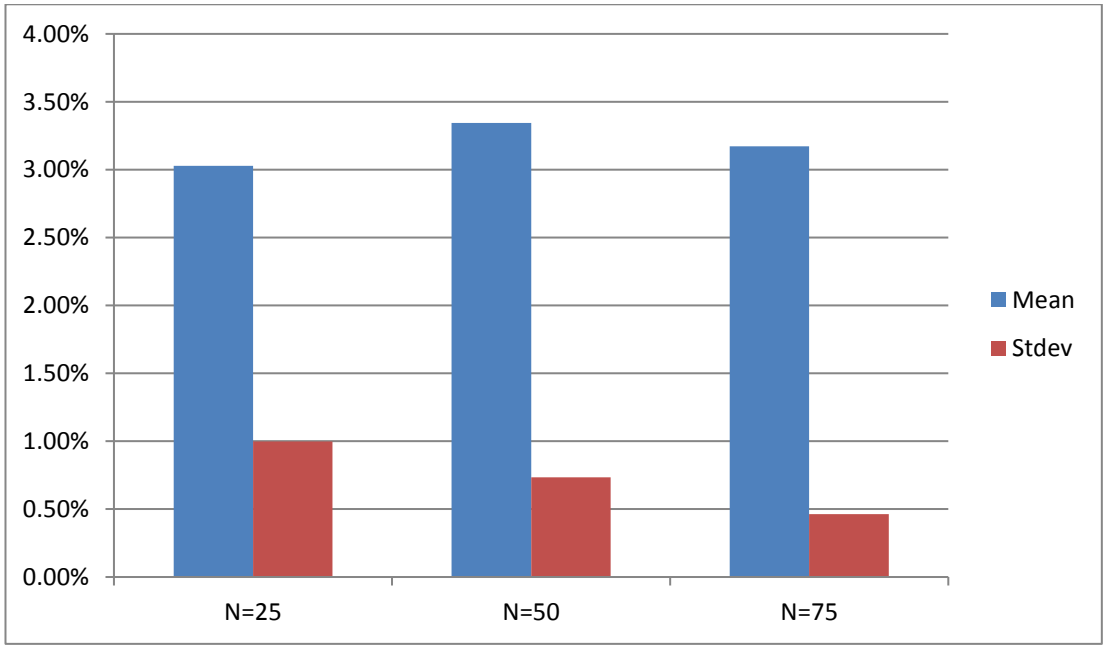

Figure 28 Mean and Standart Derivation for Trapezoidal n=7

W can notice that standart deviation of the EER decreases with increasing N.

After finishing it we compare the results of Rectangular Template with Trapezoidal Template and the results are as shown in the table below.

Table 7. Comparison of Rectangular & Trapezoidal Template

	N	ACCURACY	EER
Trapezoidal	25	99.74%	3.03%
	50	99.84%	3.34%
	75	99.89%	3.17%
	100	99.92%	2.84%
Rectangular	25	99.95%	0.78%
	50	99.96%	0.99%
	75	99.99%	0.44%
	100	99.99%	1.00%

As it is clearly seen, eventhough the difference is not big we can notice that Rectangular template gives a lower EER(Equal Error Rate) than Trapezoidal one.

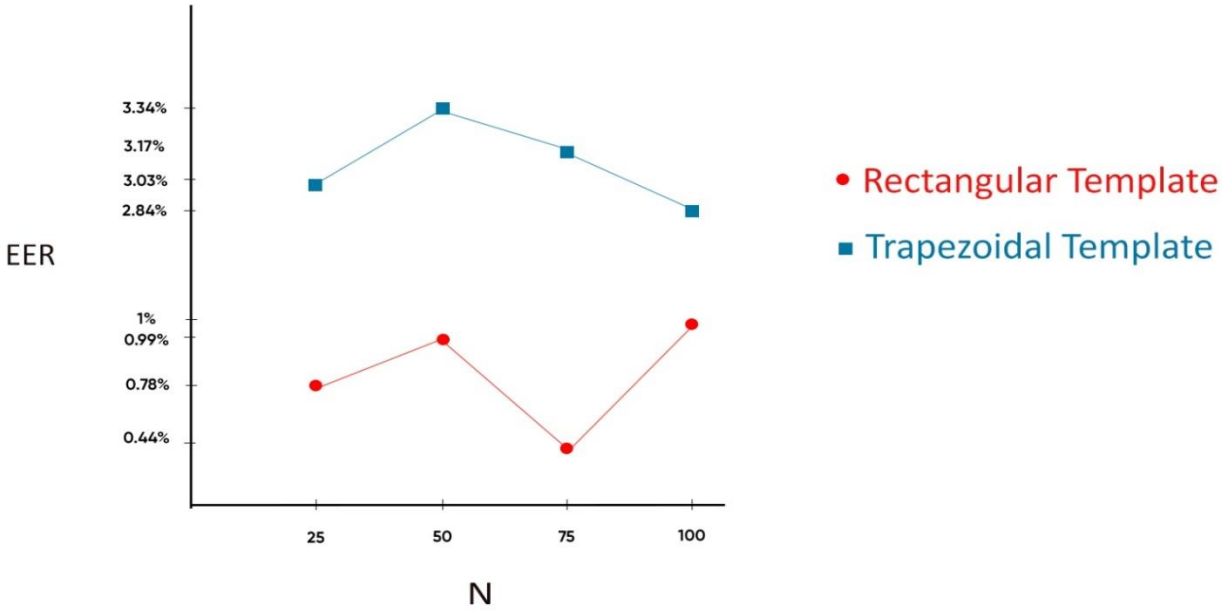

Figure 29. Comparison of Rectangular & Trapezoidal Template

After comparing them we test trapezoidal iris template by adding two different artificial noises at different noise levels; Salt-and-pepper noises and Gaussian noise

by using two segmentation types, (S1) and (S3). To decide optimum threshold values between intra and inter classes, we used classical Hamming Distance metric.When we calculate the accuracy of the iris recognition system, we have seen that the accuracy of the system with the EPK_IRIS segmentation (S3) gives always better results than classical Masek segmentation (S1) on both template types which are easily seen through.

CHAPTER 5

CONCLUSIONS

5.1 Conclusion

Our aim was to find the relation of the accuracy and EER with the number of people and the number of photos taken for each person by applying two known segmentation methods: S1 and S3 while running the experiments on two typezs of templates, rectangular and trapezoidal template. The difference between the two segmentation methods is that S1 finds first the boundary between the iris and sclera and then the boundary between the pupil and the iris, while in S3 method, the boundary between the pupil and the iris is found first. Meanwhile the difference between two types of templates is that on rectangular one we calculate using a ‘pixel intensity template’ that has a size of 20x240. While trapezoidal template uses a the ‘pixel intensity template’ that has a size of 20x936. For all the experiments we have used the CASIA database which contains images of 108 people, 7 pictures per each while changing n, N while taking random pictures from dataset

First of all, it is obvious that switching from the S1 to the S3 method of segmentation and from the E1 to the E3 method of encoding improves accuracy while maintaining the same number of subjects and the number of iris photos per subject. On the other hand, from S1 to S3 and from E1 to E3, the EER falls. This indicates that employing the S3 E3 approach with the rectangular and trapezoidal template generally results in greater efficiency.Secondly, when we apply noises to the CASIA database until 0,2% intensity we notice that on both templates all the process is done without decreasing the accuracy or increasing EER. Thirdly, we have observed a minor improvement in accuracy as well as EER when we maintain the number of iris photos per individual (n) while increasing the population (N).

In conclusion, our testing results showed that applying S3 segmentation and E3 encoding improves accuracy for rectangular and trapezoidal templates, while in rectangular template it gives better results in EER when comparing to trapezoidal

one. It is a relatively minor improvement, but when there are more than 108 people, it can have an impact. Although we can't tell for sure because of the increase in the number of people considered, more iris photos per person led to improved outcomes in the EER.

Meanwhile, we have shown the results of iris recognition system after adding two different artificial noises at different noise levels; Salt-and-pepper noises and Gaussian noises by using two segmentation types, (S1) and (S3), which are shown if Figures 6-9. When we calculate the accuracy of the iris recognition system, we have noticed that the accuracy of the system with the EPK_IRIS segmentation (S3) gives always better results than classical Masek segmentation (S1) on both templates. Also adding noises until 0.2 level did not have effect on neither of templates and the segmentation was done perfectly good.

5.2 Recommendations for future search

In this thesis we have done a variety of experiments using CASIA Database which contains iris images for 108 people, 7 iris images for each.The images are capture in the infra – red light and every eye image is saved as bitmap format and each of them has 320 x 280 pixel resolution. A future work might be to develop the same experiments but this time using other databases with same qualities as CASIA Database. This may lead to different results.

REFERENCES

1. Proença, Hugo, and Luís A. Alexandre. "UBIRIS: A noisy iris image database." *International Conference on Image Analysis and Processing*. Springer, Berlin, Heidelberg, 2005.
2. Koç, Oktay, et al. "Detailed Analysis of IRIS Recognition Performance." *2019 International Conference on Computing, Electronics & Communications Engineering (iCCECE)*. IEEE, 2019.
3. Uka, Arban, Albana Roçi, and Oktay Koç. "Improved segmentation algorithm and further optimization for iris recognition." *IEEE EUROCON 2017-17th International Conference on Smart Technologies*. IEEE, 2017.
4. Koc, Oktay, Albana Roçi, and Arban Uka. "Iris recognition and a new approach in encoding." *J. of Natural and Technical Sciences* 21.1 (2016): 89-101.
5. Koç, O., and A. Uka. "Iris recognition by 1D Fourier transform." *Proc. International Scientific Conference Computer Science*. 2015.
6. S. Qirko “Accuracy of iris recognition as a function of the size of the dataset and wavelength.” *Master Thesis at “Epoka University”* 2018.
7. Othman, Nadia, Nesma Houmani, and Bernadette Dorizzi. "Improving Video-based Iris Recognition Via Local Quality Weighted Super Resolution." *ICPRAM*. 2013.
8. Kuehlkamp, Andrey, and Kevin W. Bowyer. "An analysis of 1-to-first matching in iris recognition." *2016 IEEE Winter Conference on Applications of Computer Vision (WACV)*. IEEE, 2016.
9. Masek, Libor. *Recognition of human iris patterns for biometric identification*. Diss. master’s thesis, university of western australia, 2003.
10. Koç, Oktay, et al. "Iris Recognition Performance Analysis for Noncooperative Conditions." *2020 International Conference on Computing, Electronics & Communications Engineering (iCCECE)*. IEEE, 2020.
11. Koç, Oktay, and Arban Uka. "A new encoding of iris images employing eight quantization levels." *Journal of Image and Graphics* 4.2 (2016): 78-83.
12. Daugman, John G. "High confidence visual recognition of persons by a test of statistical independence." *IEEE transactions on pattern analysis and machine intelligence* 15.11 (1993): 1148-1161.
13. Koc, Oktay, Orges Balla, and Arban Uka. "Performance of Convolutional Neural Networks in Biometrics for Noisy Iris Images." *Proc. of the 3rd MULTI-modal Imaging of FOREnsic SciEnce Evidence Tools for Forensic Science 2019*.

14. Johar, Tania, and Pooja Kaushik. "Iris segmentation and normalization using Daugman's rubber sheet model." *International Journal of Scientific and Technical Advancements* 1.1 (2015): 11-14.

15. Koç, Oktay, Albana Roçi, and Arban Uka. "Performance analysis of iris recognition by using classical and trapezoidal shaped templates with a state-of-art iris segmentation technique." *Int. J. of Advances in Electronics and Comp. Sci.* 6.3 (2019): 64-67.

16. Rathgeb, Christian, et al. "Design decisions for an iris recognition sdk." *Handbook of iris recognition*. Springer, London, 2016. 359-396.

17. Bhattacharyya, Debnath, et al. "Biometric authentication: A review." *International Journal of u-and e-Service, Science and Technology* 2.3 (2009): 13-28.

18. Proenca, Hugo. "Iris recognition: On the segmentation of degraded images acquired in the visible wavelength." *IEEE Transactions on Pattern Analysis and Machine Intelligence* 32.8 (2009): 1502-1516.

APPENDIX

Below you can see the MATLAB files (codes), the relation to each other and the order in which they are executed.

Degrees of Freedom (DOF) code

```
aa = inter(:); % here inter means our iter-class comparision results normally these are from 0 to 1 all real numbers

b=sort(aa);

c=b(b>0);

dof=(mean(c)*(1-mean(c)))/(std(c)^2);

disp(dof);
```